# Energy & Environmental Science

Accepted Manuscript






ROYAL SOCIETY OF CHEMISTRY

www.rsc.org/ees

Cite this: DOI: 10.1039/c0xx00000x

www.rsc.org/xxxxxx

ARTICLE TYPE

# Direct synthesis of methane from $CO_2$-$H_2O$ co-electrolysis in tubular solid oxide electrolysis cells

**Long Chen,[a] Fanglin Chen[b] and Changrong Xia*[a]**

*Received (in XXX, XXX) Xth XXXXXXXXX 20XX, Accepted Xth XXXXXXXXX 20XX*

**DOI: 10.1039/b000000x**

**Directly converting $CO_2$ to hydrocarbons offers a potential route for carbon-neutral energy technologies. Here we report a novel design, integrating the high-temperature $CO_2$-$H_2O$ co-electrolysis and low-temperature Fischer-Tropsch synthesis in a single tubular unit, for the direct synthesis of methane from $CO_2$ with a substantial yield of 11.84%.**

Global advances in fossil-fuel-driven industrialization exacerbate various disquieting problems, particularly, increased scarcity of nonrenewable energy resources and heightened levels of atmospheric $CO_2$. Worldwide oil consumption has reached to more than 90 million barrels per day, and still continues to increase with a considerable rate.[1] At the same time, burning fossil fuels emits significant amount of greenhouse gas, and the concentration of atmospheric $CO_2$ has increased by 27% from 310 to 395 ppm during the past 60 years.[2] It has been widely accepted that the increased atmospheric $CO_2$ content is the major contributor to global warming and should be responsible for more and more intense weather phenomena and natural disasters. Consequently, alternative fuels and carbon-neutral energy technologies are indispensable in order to alleviate and potentially solve these energy and environmental problems. Co-electrolyzing $CO_2$ and steam using solid oxide electrolysis cells (SOECs) powered by renewable energy sources such as solar, wind, hydro, and geothermal heat is an efficient route for conversion of $CO_2$ into a syngas consisting of CO and $H_2$,[3-5] which can be further used to produce hydrocarbons with Fischer-Tropsch (F-T) process.[6] Therefore, combining SOEC and F-T processes provides not only scalable energy storage means to solve the intermittency issues related to typical renewable power sources but also an environmental friendly solution to achieve quasi-carbon neutral fuel and chemical production with recycled $CO_2$. The combination is encouraged by nickel, which is the most widely applied electrocatalyst for SOECs[7] as well as the typical methanation catalyst for F-T synthesis. Methane, the main component of natural gas, has extensive industrial uses. Consequently, integrating the two processes in a single unit creates a novel strategy to convert $CO_2$-$H_2O$ directly into methane.

However, there are technical challenges to effectively integrate the SOEC and F-T processes. High temperature (600-1000 °C) operation is preferred for SOECs due to favourable thermodynamics and kinetics considerations. The thermodynamic benefit is a decrease in the molar Gibbs energy of the reaction with an increase of temperature while the molar enthalpy remains almost the constant.[8] On the contrary, the F-T process of methanation is often conducted at low temperatures, typically 200-300 °C, to achieve high $CH_4$ yield since $CO_x$ hydrogenation is strongly exothermic and thus thermodynamically favoured at reduced temperatures. Therefore, integrating the SOEC and F-T methanation, which are favoured in different temperature ranges, in a single unit has to compromise the operation temperature. For example, 650 °C for the previously reported units.[9-11] Such temperature is selected to allow SOEC to be operated with reasonable efficiency to generate adequate syngas, but extremely impeding the methanation reaction. Consequently, only 0.2% $CH_4$ yield has been detected in a planar SOEC configuration of LSM-$Ce_{0.9}Gd_{0.1}O_{2-\delta}$/YSZ/$La_{0.2}Sr_{0.8}TiO_{3+\delta}$, where LSM is strontium doped lanthanum manganate, the electrocatalyst for the air electrode, YSZ is 8mol% yttria stabilized zirconia, the electrolyte, and $La_{0.2}Sr_{0.8}TiO_{3+\delta}$ is the catalyst for the fuel electrode.[9] A similar yield of 0.286% is reported for a planar unit of LSM-ScSZ/ScSZ/Ni-ScSZ/Ni-YSZ, in which ScYZ is scandia stabilized zirconia, the electrolyte.[11] The $CH_4$ yield has to be substantially improved for practical application.

Here we show a new design of the direct synthesis of methane from $CO_2$-$H_2O$ co-electrolysis using a tubular unit, which allows one part be controlled at high temperature for SOEC while the other at reduced temperature for F-T process (Fig. 1, see also Fig. S1 in electronic supplementary information, ESI† ). This design is capable to conduct various reactions including.

Reverse water gas shift (RWGS)

$$CO_2 + H_2 \rightarrow CO + H_2O$$

Co-electrolysis processes (SOEC)

$$2H_2O \rightarrow 2H_2 + O_2$$
$$2CO_2 \rightarrow 2CO + O_2$$

And methanation

$$CO_2 + 4H_2 \rightarrow CH_4 + 2H_2O$$
$$CO + 3H_2 \rightarrow CH_4 + H_2O$$

The design is realized using a tubular porous Ni-YSZ substrate with a dense YSZ layer. As illustrated in Fig. 1, the cell part is operated at 800 °C while the electrolysis-induced syngas can be directly catalyzed to form methane in the F-T part at temperature down to 250 °C. The design improves the $CH_4$ yield substantially to 11.84% as well as shows a stable 24 h short-term performance, demonstrating significant progress in the direct $CO_2$-$H_2O$ conversion into hydrocarbon.

The schematic diagram and experiment details for the fabrication process of the tubular units are presented in Fig. S2 and S3†. Fig. 2a presents the cross-sectional microstructure of the cell part consisting of a 310 μm thick porous Ni-YSZ fuel electrode, a 12 μm dense YSZ electrolyte and a 30 μm porous LSM-YSZ air electrode. The electrolyte is dense and has intimate bonding with the electrodes. The fuel electrode near the electrolyte is porous with fairly uniform distribution of micro size solids and pores, which provides a large number of three-phase boundaries for the electrochemical reaction. The remaining portion of the Ni-YSZ fuel electrode beneath the anode active area is very porous with some finger-like pores and microvoids. The porosity is about 55%, high enough for facile gas transportation. The unique porous structure is formed by the modified phase inversion process, mechanisms and details can be found in our previous work.[12]

The electrochemical performance is investigated in the fuel cell mode. Fig. 2b shows the performance when 20 mL $min^{-1}$ humidified hydrogen is used as the fuel and air as the oxidant. Peak power densities of 0.48, 0.36 and 0.25 W $cm^{-2}$ are obtained at 800, 750 and 700 $^{o}$C, respectively. At 800 $^{o}$C, the cell ohmic resistance is 0.36 Ω $cm^2$ while the total cell polarization resistance is 0.34 Ω $cm^2$. The cell performance is comparable with the typical tubular fuel cells prepared with the phase-inversion process.[12-14] The electrochemical performance is further investigated in the electrolysis mode at various steam concentrations using $H_2$ as the steam carrier, Fig. 2c. The cell voltage at zero current density denotes open-circuit voltage (Voc), which decreases with the increase of the steam concentration as predicted from the Nernst equation. With an applied cell voltage of 1.5 V, a current density of 0.61 A $cm^{-2}$ is observed for 20 vol.% $H_2O$ and increases to 0.83 A $cm^{-2}$ for 50 vol.% $H_2O$. Moreover, the current-voltage curves do not show any steam starvation phenomenon, demonstrating excellent gas transport property of the fuel electrode with the asymmetric porous microstructures (Fig.2a and Fig. S4†). The corresponding hydrogen production rate is also presented in Fig. 2c. The hydrogen production rate increases with the electrolysis voltage and the humidity. For example, 3.16 mL $min^{-1}$ $cm^{-2}$ hydrogen can be achieved at 1.3V and 40 vol.% humidity.

Fig.3a shows the results of $CO_2$-$H_2O$ co-electrolysis. Voc is slight lower than that for $H_2O$ electrolysis (Fig. 2c), due to the increased oxygen partial pressure by $CO_2$. The co-electrolysis performance is very close to the $H_2O$ electrolysis. For example, at 1.3V and 40% humidity, the current density is 0.47 and 0.45 A $cm^{-2}$ for the $CO_2$-$H_2O$ (Fig. 3a) and $H_2O$ (Fig. 2c), respectively. Previous research has reported that $CO_2$-$H_2O$ co-electrolysis is dominated by the steam reduction to hydrogen whereas $CO_2$ is reduced to CO by the reverse water gas shift (RWGS) reaction.15 Assuming 100% current efficiency for steam reduction, 3.24 mL $min^{-1}$ $cm^{-2}$ hydrogen can be achieved at 1.3V and 40 vol.% humidity.

The tubular unit can be used to conduct the SOEC, methanation and RWGS reactions using Ni as the catalysts (Fig. 3b). When the unit is in Position A (ESI, Fig. S1†), the F-T part and cell part are at the same temperature of 800 $^{o}$C, which is favoured for the RWGS reaction but too high for the methanation. Under the open circuit conditions, only RWGS takes place (Model I ), producing CO (15.98%) from the feeding $CO_2$-$H_2$ mixture. When the unit is under an external electrical field, both RWGS and SOEC are active (Model II). CO production is increased to 17.24% and 18.31% at 1.3V and 1.5V, respectively. As mentioned above, the improved CO production is mainly produced from the RWGS reaction through promoted $H_2$ concentration from the electrolysis process. The total $CO_2$ conversion ratio is increased by the electrolysis process from 52.7% for Model I to 66.6 and 75.4% for the Model II at 1.3 V and 1.5 V, respectively. However, no $CH_4$ component can be detected when the unit is in Position A , demonstrating that methanation reaction cannot be proceeded at 800 $^{o}$C. When it is put at Position B (ESI, Fig. S1†), the tubular unit is in a non-uniform temperature field. The cell part is at 800 $^{o}$C while the F-T part is subject to temperature gradient from 800 to 250 $^{o}$C. The reduced temperatures are favoured for methanation, and $CH_4$ (5.02%) is obtained at Voc (Model III). Much more $CH_4$ is produced when an external electrical field is applied (Model IV). The $CH_4$ yield is 11.84% at 1.3V, significantly higher than those reported using planar SOECs at a cell temperature of 650 $^{o}$C, in which the $CH_4$ yield is only 0.2-0.3%.[9, 11] The 11.84% yield means 41.0 % $CO_2$ is converted to $CH_4$ through Model IV. It should be noted that a high mechanical stability is expected in Position B although temperature gradient is applied to the F-T part, where the porous Ni-YSZ and dense YSZ have well matched thermal expansion coefficients.

For the methanation process, the increased CO and $H_2$ concentration and decreased $H_2O$ concentration are kinetically favourable. On the other hand, the reduced temperatures are thermodynamically favourable due to the exothermic process of hydrogenation. Therefore, the remarkable $CH_4$ yield is achieved using the unique design that integrates the two functional chambers in a single tubular unit. This unique design allows the SOEC chamber to operate at 800 $^{o}$C to increase the $H_2$ concentration and decrease the steam partial pressure. Furthermore, high temperature can improve the electrolysis kinetics as well. Meanwhile, the methanation chamber at reduced temperatures is thermodynamically favourable for $CH_4$ formation. Moreover, the temperature control can be easily realized with a mini-mite furnace (ESI, Fig. S1†). For scaling up test, the exhausted heat could be used to preheat the inlet $CO_2$-$H_2O$ to achieve the thermal integration.

Fig. 4 presents the short-term performance of the tubular unit operated in Model IV. (details see Tab. S1, ESI†). Fig. 4a shows that the current density decreases slightly at first and then is stabilized at 0.42 A $cm^{-2}$ with the elapsed time. Moreover, both $CH_4$ and CO show a stable yield during the test. The average $CH_4$ yield is 11.40% (0.84 mL $min^{-1}$) with the total $CO_2$ conversion ratio of 64.1%. The post tested impedance spectra and X-ray photoelectron spectroscopy also confirm the stable performance under Model IV operating conditions (ESI, Fig. S5† and Fig. S6†). Meanwhile, the by-product (CO-$H_2$ syngas) is also highly valuable and can be further cycled to improve methane yield. Higher hydrocarbons yield may be obtained by further improving the F-T synthesis conditions, such as employing high-efficiency methanation catalysts.

## Conclusions

In this work, we have demonstrated a tubular design for direct synthesis of $CH_4$ from $CO_2$-$H_2O$ feedstock. This unique design substantially improve $CH_4$ yield to 11.84% by combining the $CO_2$-$H_2O$ co-electrolysis and methanation in a single tubular unit. 24h short-term test shows that the co-electrolysis process presents a generally stable current density at 0.42 A $cm^{-2}$ during the electrolysis operation while the average $CH_4$ yield can reach 11.40% (0.84 mL min-1) with an overall $CO_2$ conversion ratio of 64.1%. The novel integration of $CO_2$-$H_2O$ co-electrolysis and methanation in a single tubular unit presents a significant advancement in hydrogen economy and a carbon neutral renewable energy cycle.

## Acknowledgements

We greatly appreciate supports from the National Natural Science Foundation of China (51372239), the Ministry of Science and Technology of China (2012CB215403) and the U.S. National Science Foundation (DMR-1210792).

## Notes and references

[a] *CAS Key Laboratory of Materials for Energy Conversion, Department of Materials Science and Engineering & Collaborative Innovation Center of Suzhou Nano Science and Technology, University of Science and Technology of China, Hefei, Anhui 230026, China. Fax: 86 551 63601696; Tel: 86 551 63607475; E-mail: xiacr@ustc.edu.cn*

[b] *Department of Mechanical Engineering, University of South Carolina, Columbia, SC 29208, USA. Fax: 1 803 7770106; Tel: 1 803 7774875; E-mail: CHENFA@cec.sc.edu*

† Electronic Supplementary Information (ESI) available: Fig. S1-S6, Schematic diagram for working principle of tubular unit, fabrication and characterization of tubular unit, data details for the unit operated under different models, impedance spectra and XPS anlysis after 24 h short-term test. See DOI: 10.1039/b000000x/

1. U. S. E. I. A. (EIA), Short-term Energy Outlook, http://www.eia.gov/forecasts/steo/index.cfm, Accessed August 12, 2014.
2. M. McGee, 399.00ppm: Atmospheric $CO_2$ for July 2014, http://co2now.org/, Accessed August 6, 2014.
3. Q. X. Fu, C. Mabilat, M. Zahid, A. Brisse and L. Gautier, *Energy Environ. Sci.*, 2010, **3**, 1382-1397.
4. C. Graves, S. D. Ebbesen, M. Mogensen and K. S. Lackner, *Renew. Sust. Energ. Rev.*, 2011, **15**, 1-23.
5. K. Christopher and R. Dimitrios, *Energy Environ. Sci.*, 2012, **5**, 6640-6651.
6. G. P. Van Der Laan and A. A. C. M. Beenackers, *Catal. Rev.-Sci. Eng.*, 1999, **41**, 255-318.
7. T. Ishihara, N. Jirathiwathanakul and H. Zhong, *Energy Environ. Sci.*, 2010, **3**, 665-672.
8. L. Bi, S. Boulfrad and E. Traversa, *Chem. Soc. Rev.*, 2014, **DOI: 10.1039/c4cs00194j**.
9. K. Xie, Y. Q. Zhang, G. Y. Meng and J. T. S. Irvine, *Energy Environ. Sci.*, 2011, **4**, 2218-2222.
10. K. Xie, Y. Q. Zhang, G. Y. Meng and J. T. S. Irvine, *J. Mater. Chem.*, 2011, **21**, 195-198.
11. W. Y. Li, H. J. Wang, Y. X. Shi and N. S. Cai, *Int. J. Hydrogen Energy*, 2013, **38**, 11104-11109.
12. L. Chen, M. T. Yao and C. R. Xia, *Electrochem. Commun.*, 2014, **38**, 114-116.
13. C. L. Yang, W. Li, S. Q. Zhang, L. Bi, R. R. Peng, C. S. Chen and W. Liu, *J. Power Sources*, 2009, **187**, 90-92.
14. C. H. Yang, C. Jin and F. L. Chen, *Electrochim. Acta*, 2010, **56**, 80-84.
15. Z. L. Zhan and L. Zhao, *J. Power Sources*, 2010, **195**, 7250-7254.

Cite this: DOI: 10.1039/c0xx00000x

www.rsc.org/xxxxxx

# ARTICLE TYPE

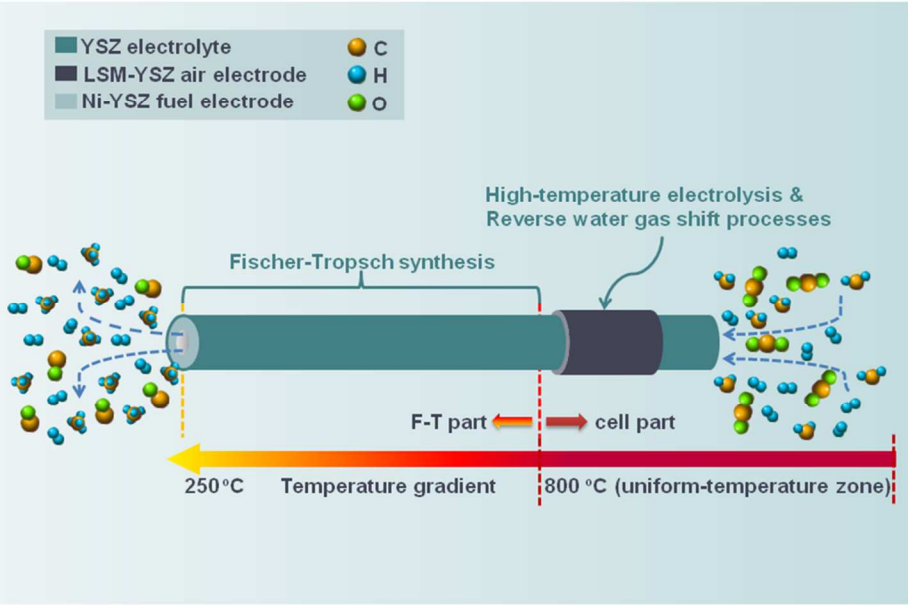


Fig. 1. Illustration for direct methane synthesis from $CO_2$-$H_2O$ co-electrolysis in a tubular unit combining an high-temperature SOEC and a reduced temperature Fischer-Tropsch reactor.

Fig. 2. Microstructures and performances for the LSM-YSZ/YSZ/Ni-YSZ tubular unit.

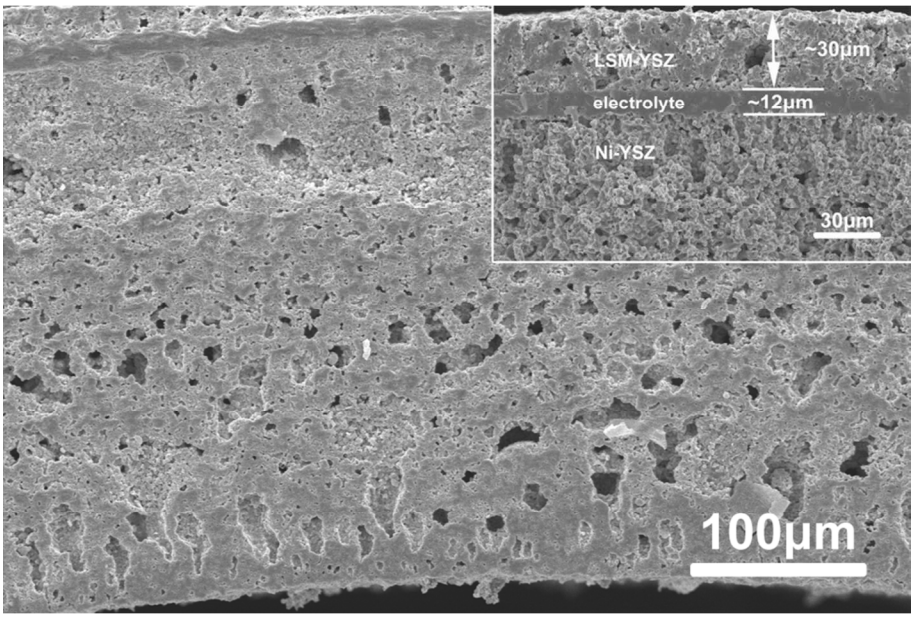


Fig. 2a Cross-sectional SEM pictures of a tested cell. The up-right picture is the enlarged microview showing the electrode-electrolyte interfaces.

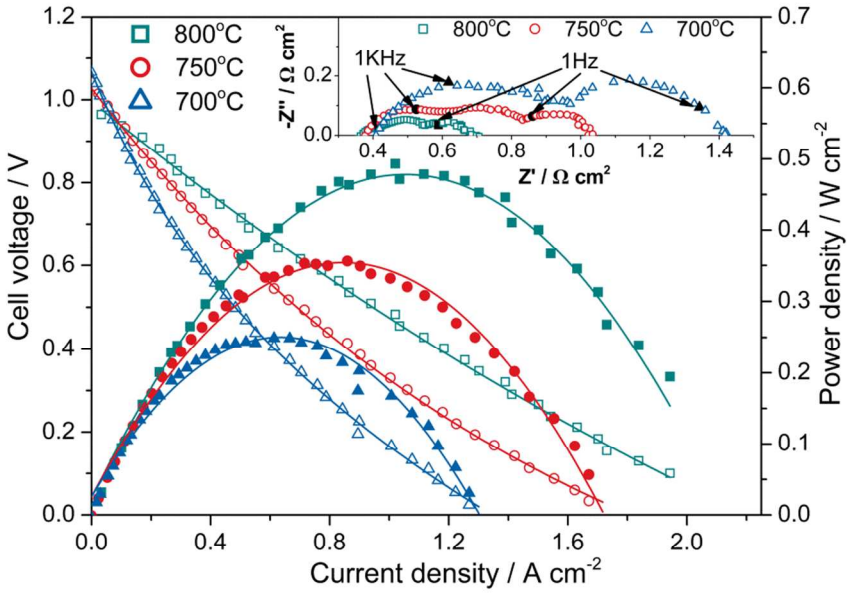


Fig. 2b Cell voltage and power density as a function of current density in the fuel cell mode with 20 mL $min^{-1}$ $H_2$ (2vol.% $H_2O$) as the fuel. The Inset is the impedance spectra.

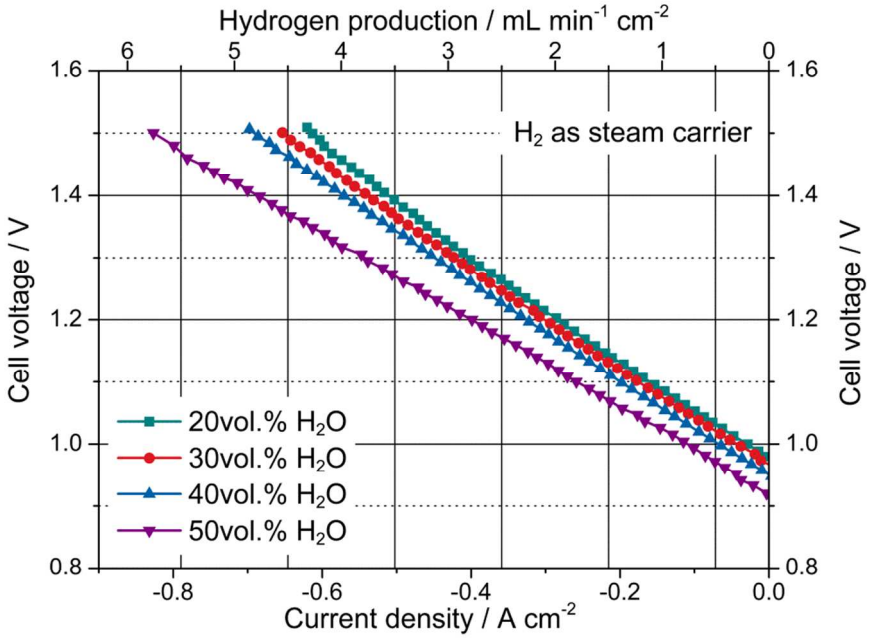


Fig. 2c I-V curves and corresponding hydrogen production in the electrolysis mode obtained at different humidity and 800 $^{o}$C using 20mL min$^{-1}$ $H_2$ as the steam carrier.

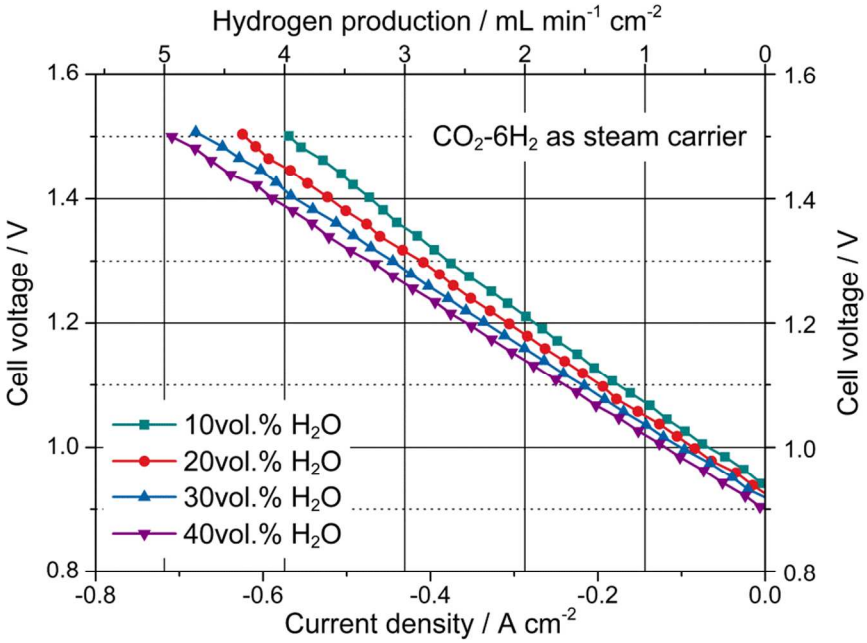


Fig. 3a I-V curves and corresponding hydrogen production in the electrolysis mode obtained at different humidity and 800 °C using ~15 mL min$^{-1}$ $CO_2$-$H_2$ (1:6, volume ratio) mixture as the steam carrier.

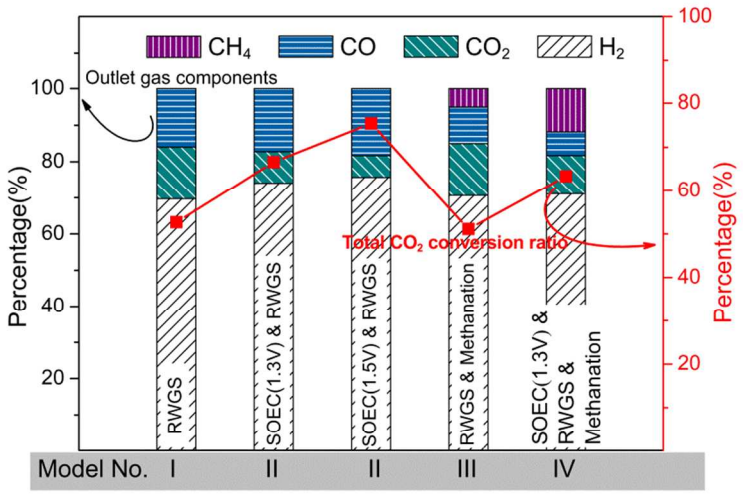


Fig. 3b Component percentage in the outlet gas and total $CO_2$ conversion ratio under different operation conditions. Model I: Position A (ESI, Fig. S1†, the whole unit is subjected to 800 °C), Voc, RWGS process only; Model II: Position A, external voltage applied, SOEC and RWGS processes; Model III; Position B (ESI, Fig. S1†, uniform 800 °C zone for SOEC part, 800-250 °C temperature gradient for F-T part), Voc, RWGS and methanation processes; Model IV: Position B, 1.3V external voltage, SOEC, RWGS and methanation processes. The inlet gas is ~15 mL min$^{-1}$ $CO_2$-$H_2$ (1:6, volume ratio) mixture with 20vol.% humidity.

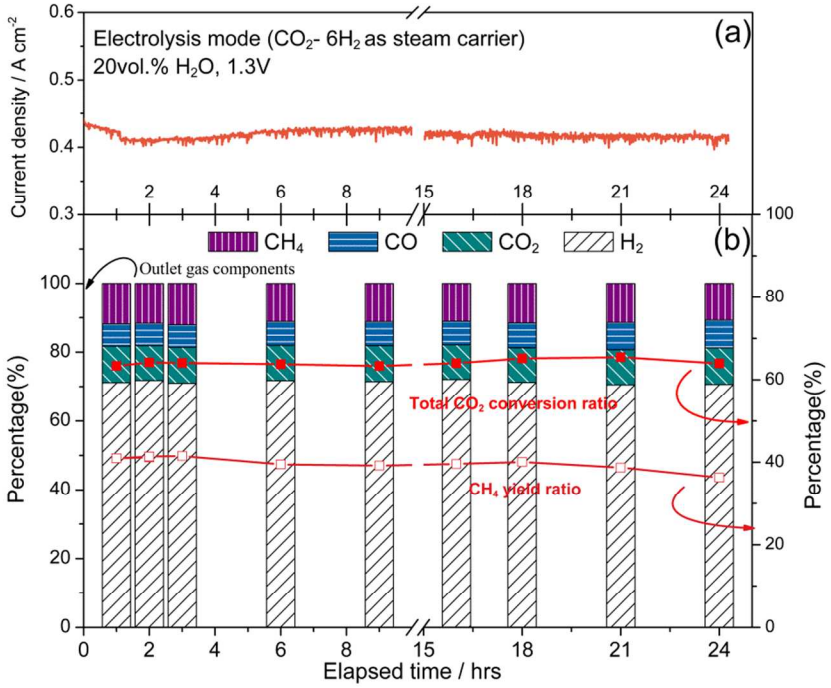


Fig. 4 Performance of a tubular unit operated in Model IV at 1.3V. The inlet steam carrier is ~15mL min$^{-1}$ $CO_2$-$H_2$ (1:6, volume ratio) with the relative humidity of 20%. (a) current density; (b) outlet gas components, total $CO_2$ conversion ratio and $CH_4$ yield ratio versus elapsed time.